Optical Study of the Free-Carrier Response of $LaTiO_3/SrTiO_3$ Superlattices

S. S. A. Seo,[1,*] W. S. Choi,[1] H. N. Lee,[2] L. Yu,[3] K. W. Kim,[3] C. Bernhard,[3] and T. W. Noh[1,†]

We used infrared spectroscopic ellipsometry to investigate the electronic properties of $LaTiO_3/SrTiO_3$ superlattices (SLs). Our results indicated that, independent of the SL periodicity and individual layer thickness, the SLs exhibited a Drude metallic response with sheet carrier density per interface $\approx 3 \times 10^{14}$ cm^{-2}. This is probably due to the leakage of d electrons at interfaces from the Mott insulator $LaTiO_3$ to the band insulator $SrTiO_3$. We observed a carrier relaxation time ≈ 35 fs and mobility ≈ 35 cm^2 V^{-1} s^{-1} at 10 K, and an unusual temperature dependence of carrier density that was attributed to the dielectric screening of quantum paraelectric $SrTiO_3$.

PACS numbers: 73.20.−r, 71.27.+a, 73.40.−c, 78.67.Pt

Recent advances in the growth of atomic-scale multilayers of perovskites have opened up new avenues for tailoring their electromagnetic properties. For example, Ohtomo *et al.* grew superlattices (SLs) consisting of an $LaTiO_3$ (LTO) Mott insulator and an $SrTiO_3$ (STO) band insulator with atomically abrupt interfaces (IFs) [1]. They observed an interesting charge modulation involving electron transfer across the IF from the LTO to the STO layers. This had a decay length of 1.0 ± 0.2 nm, which is about 1 order of magnitude larger than expected for conventional Thomas-Fermi screening. Subsequent transport measurements have been interpreted in terms of an unusual metallic state with quasi-two-dimensional properties. This intriguing experimental observation has stimulated a number of theoretical investigations [2–5], which confirm that so-called ''electronic reconstruction'' [2] can indeed give rise to a unique interfacial metallic state.

There is now a great deal of demand for experimental confirmation and direct investigation of such interfacial metallic states. Takizawa *et al.* recently measured photoemission spectra of LTO/STO SLs with a topmost STO layer of variable thickness [6]. They observed a metallic Fermi edge, indicating the formation of a metallic IF. However, to date there have been no reports of quantitative experimental information on the electrodynamic properties of the itinerant electrons. Here, we present spectroscopic ellipsometry measurements of the infrared (IR) dielectric properties for a set of (LTO)α/(STO)10 SLs with $\alpha = 1$, 2, 4, and 5 unit cells of LTO layer and 10 unit cells of STO. Our IR optical data yield reliable information about the intrinsic electrodynamic properties of these SLs. First, they clearly demonstrate that these SLs contain a sizable concentration of itinerant charge carriers. Furthermore, they establish that the sheet carrier density is proportional to the number of IFs, and its absolute value agrees closely with the theoretical predictions. Our data also highlight an unusually strong temperature (T) dependence of the carrier density, which was unexpected for bulk metals, but can be explained in terms of the T-dependent dielectric screening of the STO layer controlling charge transfer across the LTO/STO IF.

We grew high-quality LTO/STO SLs ~100 nm thick with atomically flat surfaces and abrupt IFs on single crystalline STO (001) substrates. To do this, we used pulsed laser deposition (PLD) at $T = 720\,^{\circ}$C in $P_{O2} = 10^{-5}$ Torr with *in situ* monitoring of the specular spot intensity of reflection high-energy electron diffraction (RHEED) (see Ref. [7] for more details on PLD growth). The RHEED intensity oscillations in Fig. 1(a) confirmed the controlled growth of alternating LTO and STO layers. Doing this at a higher oxygen pressure would result in the growth of unwanted $La_2Ti_2O_7$ phases, as reported previously [8]. After growth, all samples were exposed immediately to a higher pressure ($P_{O2} = 10^{-2}$ Torr) for *in situ* postannealing at growth T for 5 min, and then cooled to room T. No changes in the RHEED specular spot pattern were observed after postannealing. The atomic force microscope topographic image in Fig. 1(b) shows that the SLs retained

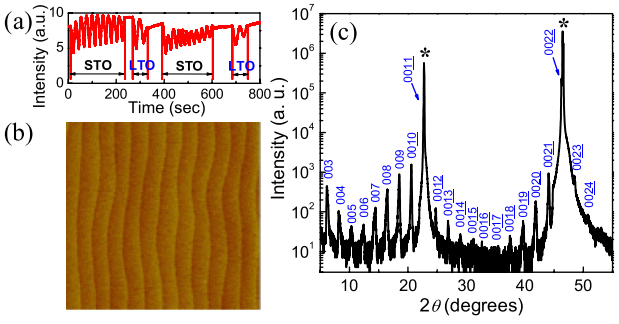

FIG. 1 (color online). (a) RHEED intensity oscillation during the initial growth of the (LTO)2/(STO)10 SL. (b) Atomic force microscope topographic image ($5 \times 5\ \mu$m^2) of an (LTO)1/(STO)10 SL 100 nm thick with single unit cell terraces conserved. (c) X-ray θ-2θ scan of (LTO)1/(STO)10. Peaks marked with (*) are reflected from the STO substrate.

their single unit cell terrace steps even after deposition of ~250 unit cells of LTO and STO. Figure 1(c) shows x-ray θ-2θ diffraction, exhibiting well-defined satellite peaks, confirming the high IF quality and SL periodicity of LTO and STO layers. The full-width half-maximum $\leq 0.04°$ in ω scan, which is almost identical to the substrate scan, confirmed the high crystallinity of the SLs.

We measured the T-dependent IR optical properties of the SLs using ellipsometry in the range of 80–5000 cm^{-1} (10–600 meV). The far-infrared (FIR) measurements for 80–700 cm^{-1} were performed with a homebuilt ellipsometer attached to a Bruker 66v Fourier transform IR (FT-IR) spectrometer at the IR beam line of the ANKA synchrotron at FZ Karlsruhe, Germany [9]. For the mid-infrared (MIR) range of 400–5000 cm^{-1}, we used a homebuilt ellipsometer in combination with the glow-bar source of a Bruker 113v FT-IR spectrometer. The FIR (MIR) measurement was performed with an angle of incidence of the linearly polarized light of 82.5° (80°), i.e., close to the pseudo-Brewster angle of the SLs. Details about the ellipsometry technique are given in Refs. [9,10]. Here, we point out only that the ellipsometry is a self-normalizing technique that directly measures the complex dielectric function $\tilde{\varepsilon}(\omega)$ $[=\varepsilon_1(\omega) + i\varepsilon_2(\omega)]$, without the need for Kramers-Kronig analysis. We also measured the T-dependent spectroscopic response of a bare STO substrate that was treated thermally under the same growth and annealing conditions of T and P_{O2} as the SLs. Then we used a uniaxially anisotropic single-layer model [10] to obtain the in-plane component [11] of $\tilde{\varepsilon}(\omega)$, and the related optical conductivity $\tilde{\sigma}(\omega)$ $[=\tilde{\varepsilon}(\omega)\omega/4\pi i = \sigma_1(\omega) - i\varepsilon_1(\omega)\omega/4\pi]$ of the SLs. As the thickness of the SLs is well below our IR wavelength, the entire SL film can be treated as a single layer according to the effective medium theory. The resulting effective dielectric functions thus correspond to the volume-averaged dielectric functions of the components in the SL. Our optical technique can provide intrinsic values

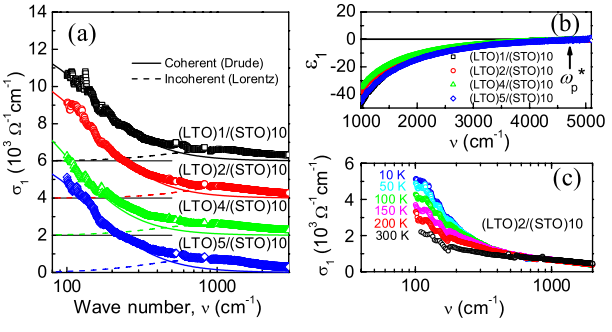

FIG. 2 (color online). (a) Optical conductivity spectra of (LTO)α/(STO)10 at 10 K (with vertical offsets), containing the coherent (Drude) and incoherent (Lorentz) contributions. (b) SL real dielectric constant spectra as a function of photon wave number at 10 K. The arrow indicates the screened plasma frequency $\omega_p^*[=\omega_{pD}/\sqrt{\varepsilon_\infty}]$. (c) T-dependent $\sigma_1(\omega)$ of (LTO)2/(STO)10.

of the bulk properties of these SLs, which can be compared with the preexisting results of transport measurements [1].

Figures 2(a) and 2(b) show the low-T spectra of $\sigma_1(\omega)$ and $\varepsilon_1(\omega)$ for the series of (LTO)α/(STO)10 SLs with $\alpha = 1, 2, 4$, and 5. Significantly, all the spectra exhibited a prominent Drude-like peak at low frequency in $\sigma_1(\omega)$ and a strongly inductive response in $\varepsilon_1(\omega)$, which provided unambiguous evidence that these SLs contained sizable concentrations of itinerant charge carriers. The strongly conducting response also seemed to damp out IR active phonons in the spectra. For quantitative analysis we applied the Drude-Lorentz fitting function:

$$\tilde{\varepsilon}(\omega) = \varepsilon_\infty - \frac{\omega_{pD}^2}{\omega^2 + i\omega\Gamma_D} + \frac{S\omega_0^2}{\omega_0^2 - \omega^2 - i\omega\Gamma}. \quad (1)$$

This is shown in Fig. 2(a) by the solid and dashed lines. The parameters of the Drude term are the scattering rate Γ_D, and the plasma frequency $\omega_{pD}^2 = 4\pi ne^2/m^*$, where n, e, and m^* are the density, charge, and effective mass of the itinerant charge carriers, respectively. The parameters of the Lorentz term that accounts for the broad MIR band are the oscillator strength S, the width Γ, and the resonant frequency ω_0. A broad MIR band is commonly observed in conducting oxides and has been interpreted in terms of either the inelastic interaction of the itinerant carriers, a second type of carrier in a bound state, or low-lying interband transitions. As LTO is well known to have weak broad MIR bands, the Lorentz peak with a small value of S can be reasonably interpreted to be the lowest intersite d-d (i.e., U-3J) transition of LTO [12]. An overview of the fitting parameters for the low-T spectra is given in Table I.

Most importantly, we noted that all the SLs have surprisingly high ω_{pD}, and thus high densities of free carriers. This observation motivated us to follow up on suggestion of Okamoto and Millis [2] of a quasi-two-dimensional metallic state that develops in the LTO/STO IFs. We derived the sheet carrier density per IF, $n_{\text{sheet}} = n\frac{d}{N_I}$, with the total SL thickness d and the number of LTO/STO IFs N_I of the SL [13]. Figure 3(a) shows n_{sheet} values within error bars dependent on the detailed assignment of m^* based on the analysis of our ellipsometric data in the framework of the extended Drude- model. This directly yields the renormalized mass $m^*/m_e = (\omega_p/\omega)^2(\varepsilon_0 - \varepsilon_1)/[(\varepsilon_0 - \varepsilon_1)^2 - \varepsilon_2^2]$. Note that all of our SLs exhibit a very similar value of

TABLE I. Drude-Lorentz fitting parameters for optical spectra of (LTO)α/(STO)10 SLs measured at 10 K.

	Drude		Lorentz		
α	ω_{pD}^2 (cm^{-1})	Γ_D (cm^{-1})	S	ω_0 (cm^{-1})	Γ (cm^{-1})
1	6.0×10^7	128(±3)	75(±11)	920(±95)	1980(±580)
2	6.6×10^7	144(±8)	51(±22)	980(±240)	1530(±1200)
4	5.1×10^7	105(±6)	87(±20)	780(±200)	1630(±1000)
5	6.1×10^7	122(±2)	126(±8)	750(±65)	1740(±350)

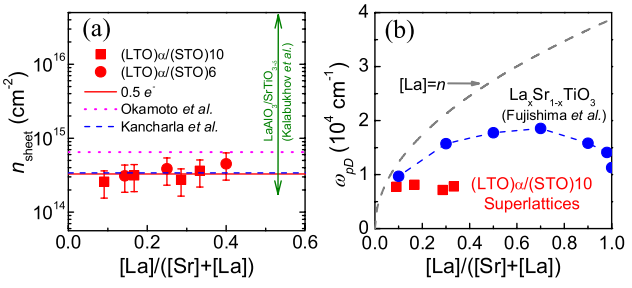

FIG. 3 (color online). (a) $n_{\rm sheet}$ per IF. The solid line indicates the value of an ideal 0.5 e^- per unit cell area, and the dashed and dotted lines represent theoretically predicted values reported by Kancharla [5] and Okamoto [3], respectively. The vertical arrow shows the range of $n_{\rm sheet}$ in $LaAlO_3/SrTiO_{3-\delta}$ IF from Ref. [23]. (b) Comparison of SL ω_{pD} with solid solution [17] and the ideal doping of [La] = n as a function of La and Sr composition.

$n_{\rm sheet} \approx 3 \times 10^{14}$ cm^{-2} with $m^* = 1.8m_e$ [14], which agrees well with theoretical predictions [3,5,15].

Here, we should mention that the Drude term is only a phenomenological description, and its microscopic origin is not clear. One possible explanation is in terms of a chemical intermixing of La and Sr ions across the IFs because $La_xSr_{1-x}TiO_3$ solid solutions are metallic [16]. As indicated by the solid circles in Fig. 3(b), the experimental data of bulk $La_xSr_{1-x}TiO_3$ solid solutions reported by Fujishima *et al.* [17] show that the ω_{pD} value increases from $x = 0.1$ to 0.7, while it decreases above 0.7 due to the strong electron correlation effect as a function of increasing x. However, our SL data follow a different path although the value of ω_{pD} is expected to increase when going from $\alpha = 1$ to $\alpha = 5$, as shown by the solid squares in Fig. 3(b). Moreover, the well-defined superstructure peaks in our x-ray diffraction data and the abrupt IFs seen on cross-sectional transmission electron microscopy (not shown) confirm that the extent of La and Sr intermixing is negligible.

As other candidates of extrinsic origin, it is also necessary to consider the possibility of oxygen excess $LaTiO_{3+\delta}$ [18] or La vacancy $La_{1-x}TiO_3$ [19] of LTO, and oxygen deficiency of STO [20]. The former possibility can be excluded as our data for ω_{pD} do not exhibit a corresponding change as the relative volume fraction of the LTO layers is altered by a factor of 5 between $\alpha = 1$ and 5. On the other hand, serious consideration should be given to the latter possibility of oxygen deficiency and thus metallic $SrTiO_{3-\delta}$ layers. It is noteworthy that numerous recent controversial studies and some debate in oxide electronics circles have centered on the discontinuous IF polarity of $LaAlO_3/STO$ [21] especially regarding the origin of conduction due to the oxygen vacancies [22]. As indicated by the arrow in Fig. 3(a), the range of $n_{\rm sheet}$ values of $LaAlO_3/SrTiO_{3-\delta}$ grown at low oxygen pressure [23] is so wide that it also overlaps our experimental value of $n_{\rm sheet} \approx 3 \times 10^{14}$ cm^{-2} as well as with the theoretical values [3,5] of electronic reconstruction at the LTO/STO IF. However, according to the recent report by Herranz *et al.*, $LaAlO_3/STO$ films were all insulating or highly resistive when cooled in a high oxygen pressure environment from the deposition T to room T [24]. We performed a similar *in situ* oxygen annealing process to compensate for possible oxygen vacancies, but our LTO/STO SLs still exhibited metallic behavior.

Another interesting aspect concerns the strong T dependence of $n(T)$. Figure 2(c) shows the T dependence of $\sigma_1(\omega)$ for (LTO)2/(STO)10, which are characteristic of all SLs. Figure 4(a) shows that $n(T)$ increased significantly by almost 30% between 300 K and 10 K. The corresponding $n(T)$ in a conventional normal metal is typically of the order of 1%, even for oxides with strongly correlated electrons. For the cuprate high-T_c superconductors, for example, it is smaller than 10% [25]. Even the opposite T dependence is observed for doped semiconductors where $n(T)$ decreases as the carriers become trapped at low T. Thus, the increase of $n(T)$ at low T also cannot be explained by the electron-doping effect of oxygen vacancies of STO. However, we note that the quantum paraelectric behavior of incipient ferroelectric STO exhibits a significant increase in dielectric permittivity ($\epsilon_0^{\rm STO}$) as T decreases. Therefore, we can explain the increase of $n(T)$ in the context of electronic reconstruction at an IF. The charge transfer across the IF of LTO/STO (and thus $n_{\rm sheet}$) should be affected by the dielectric screening of the STO layer. The larger value of $\epsilon_0^{\rm STO}$ thus gives rise to the larger screening length of the electronic charges, and this allows more charges to be transferred across the LTO/STO IF. (See also the theoretical prediction of the coherent carrier density as a function of ϵ_0 by Kancharla [5].)

Figure 4(b) displays the relaxation time of free carriers $\tau(T)[= \Gamma_D^{-1}(T)]$. As all of our LTO/STO SLs showed a significantly reduced Γ_D, which is at least 1 order of magnitude smaller than a doped Mott system [26], fairly high mobility $\mu(10\ {\rm K}) \approx 35\ {\rm cm^2\,V^{-1}\,s^{-1}}$ was obtained according to the relation $\mu = e\tau/m^*$ with $m^* = 1.8m_e$. It would be interesting to consider whether signatures of novel phenomena, such as the quantum Hall effect, may be observable in the LTO/STO SLs. The measured value of $\tau \approx 3.5 \times 10^{-14}$ s at 10 K yields $\omega_c\tau = 0.01$–0.02, where the cyclotron frequency $\omega_c = eB/m^*$ with the magnetic

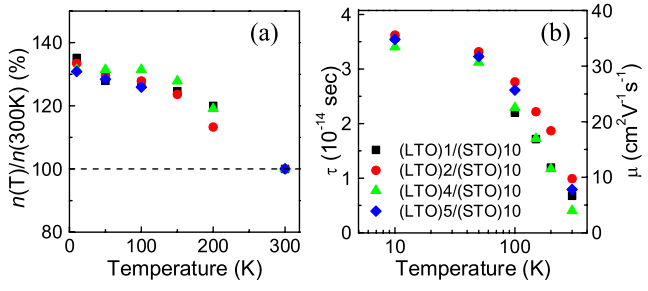

FIG. 4 (color online). T dependence of (a) the carrier density, and (b) the relaxation time and mobility of free carriers for (LTO)α/(STO)10 SLs.

field $B \approx 20$ T and $m^* = 1.0$–$2.5 m_e$. From the obtained carrier density and mobility of our LTO/STO SLs, we determined that the mean free path of the conducting electrons is about 10 nm ($\approx$25 unit cells long) at 10 K. It is remarkable that there was a recent observation of the quantum Hall effect in ZnO-based heterostructures below 1 K [27], in which the coherence length of the electron was considerably longer than those in other oxides.

In summary, our use of IR spectroscopic ellipsometry showed that all the LTO/STO SLs exhibited a Drude-like metallic response regardless of the SL periodicity and the individual layer thicknesses, even after *in situ* postannealing in oxygen. Our data yielded a nearly constant n_{sheet} per IF of $\sim 3 \times 10^{14}$ cm^{-2} with small Γ_D of $\sim$120 cm^{-1}, and a sizable mean free path of $\sim$25 unit cells at 10 K. We note that the unusually strong T dependence of n can be interpreted qualitatively as quantum paraelectric behavior of STO with theoretical prediction of the leakage of d electrons from LTO to STO across the IF. A picture of electron doping by the oxygen vacancy of STO, which has been the subject of recent debate on similar systems of $LaAlO_3$/STO, is insufficient to explain our observations in LTO/STO SLs. Hence, we note the difference between an LTO Mott insulator and an $LaAlO_3$ band insulator, and suggest that the strongly correlated d electrons of LTO should play an important role in electronic reconstruction and the resultant metallic state at a polar (LTO) and nonpolar (STO) oxide IF.

The authors thank S. Okamoto, A. J. Millis, H. Y. Hwang, G. W. J. Hassink, J. S. Ahn, D.-W. Kim, Y. S. Lee, J. Yu, K. Char, K. H. Kim, J. H. Park, J. Y. Kim, J. S. Kim, A. V. Boris, and B. Keimer for valuable discussions, as well as Y. L. Mathis for support at IR-BL of ANKA. This work was supported by the Creative Research Initiatives (Functionally Integrated Oxide Heterostructure) of KOSEF, the Swiss National Science Foundation (SNF Project No. 200021-111690/1), and the Division of Materials Sciences and Engineering, U.S. Department of Energy (H. N. L.). Experiments in PLS were supported by MOST and POSTECH.

*Present address: Max-Planck-Institute for Solid State Research, 70569 Stuttgart, Germany.

†twnoh@snu.ac.kr

[1] A. Ohtomo *et al.*, Nature (London) **419**, 378 (2002).
[2] S. Okamoto and A. J. Millis, Nature (London) **428**, 630 (2004).
[3] S. Okamoto and A. J. Millis, Phys. Rev. B **70**, 241104(R) (2004).
[4] S. Okamoto and A. J. Millis, Phys. Rev. B **70**, 075101 (2004); S. Okamoto and A. J. Millis, *ibid.* **72**, 235108 (2005); S. Okamoto and A. J. Millis, Physica B, Condens. Matter **359**, 1378 (2005); S. Okamoto, A. J. Millis, and N. A. Spaldin, Phys. Rev. Lett. **97**, 056802 (2006); Z. S. Popovic and S. Satpathy, *ibid.* **94**, 176805 (2005).
[5] S. S. Kancharla and E. Dagotto, Phys. Rev. B **74**, 195427 (2006).
[6] M. Takizawa *et al.*, Phys. Rev. Lett. **97**, 057601 (2006).
[7] H. N. Lee *et al.*, Nature (London) **433**, 395 (2005).
[8] A. Ohtomo *et al.*, Appl. Phys. Lett. **80**, 3922 (2002).
[9] C. Bernhard, J. Humlicek, and B. Keimer, Thin Solid Films **455–456**, 143 (2004).
[10] R. M. A. Azzam and N. M. Bashara, *Ellipsometry and Polarized Light* (North-Holland, Amsterdam, 1987).
[11] Okamoto *et al.* [3] suggested sharp optical transitions along the c axis due to bound states of quantum well-like structures in the IR energy region (with $t \sim 0.3$ eV). However, the large refractive indices (>10) due to conducting IFs make the refraction angle $\leq 5°$. Therefore, the electric field of infrared waves is almost parallel to the in-plane direction, and it allows discussion of the in-plane response only.
[12] J. S. Lee, M. W. Kim, and T. W. Noh, New J. Phys. **7**, 147 (2005).
[13] For (LTO)1/(STO)10 and (LTO)1/(STO)6, it is rather ambiguous to define the number of IF. Here, we count two IFs (both sides) per LTO layer for consistency with other SL samples. Hence, the n_{sheet} of (LTO)1/(STO)10 and (LTO)1/(STO)6 may be reduced due to overestimated N_I.
[14] Note $m^* = 1.62 m_e$ from the thermoelectric experiment for $La_xSr_{1-x}TiO_3$ by T. Okuda *et al.*, Phys. Rev. B **63**, 113104 (2001).
[15] The values from the theoretical calculations of $\sim 6.5 \times 10^{14}$ cm^{-2} and $\sim 3.4 \times 10^{14}$ cm^{-2} are obtained by integrating the coherent d-electron density curves displayed in Figs. 2 and 2(a) of Refs. [3,5], respectively.
[16] Y. Tokura *et al.*, Phys. Rev. Lett. **70**, 2126 (1993).
[17] Y. Fujishima *et al.*, Phys. Rev. B **46**, 11167 (1992).
[18] A. Schmehl *et al.*, Appl. Phys. Lett. **82**, 3077 (2003).
[19] D. A. Crandles *et al.*, Phys. Rev. B **49**, 16207 (1994).
[20] D. A. Crandles *et al.*, Phys. Rev. B **59**, 12842 (1999).
[21] A. Ohtomo and H. Y. Hwang, Nature (London) **427**, 423 (2004).
[22] J. N. Eckstein, Nat. Mater. **6**, 473 (2007).
[23] A. Kalabukhov *et al.*, Phys. Rev. B **75**, 121404(R) (2007).
[24] G. Herranz *et al.*, Phys. Rev. Lett. **98**, 216803 (2007).
[25] A. Toschi *et al.*, Phys. Rev. Lett. **95**, 097002 (2005).
[26] T. Katsufuji, Y. Okimoto, and Y. Tokura, Phys. Rev. Lett. **75**, 3497 (1995).
[27] A. Tsukazaki *et al.*, Science **315**, 1388 (2007).